Butterfly wing iridescence is regulated by *araucan*, a direct target of optix and spalt

Martik Chatterjee[1], Kate J. Siegel[1], Ling Sheng Loh[2] , Jeanne M.C. McDonald[1] and Robert D. Reed[1]

[1]Department of Ecology and Evolutionary Biology, Cornell University, Ithaca, NY,14853

[2]Department of Biological Sciences, Colombian College of Arts and Sciences, George Washington University, Washington, D.C, 20052

Correspondence

Robert D. Reed, Department of Ecology and Evolutionary Biology, Cornell University, 215 Tower Road, Ithaca, NY, 14853

Email: robertreed@cornell.edu

Martik Chatterjee, Department of Ecology and Evolutionary Biology, Cornell University, 215 Tower Road, Ithaca, NY, 14853

Email: mc2548@cornell.edu

Funding Information

National Science Foundation, Award Numbers IOS 2128164 and DEB 2242865 to RDR.

ABSTRACT

Butterfly wings are notable for the diversity of structural colors they display, including many striking hues of iridescence. Little is known, however, about how iridescent coloration is genetically determined. Here we show that the *Iroquois*-complex transcription factor *araucan* has a highly specific effect on wing scale iridescence hue in the common buckeye butterfly, *Junonia coenia*. CRISPR knockouts of *araucan* cause dorsal wing scales to shift from gold to blue iridescence, and eyespot focus scales to shift from purple iridescence to colorless. These effects are associated with a change in thickness in the scale cell basal lamina, as also seen in knockouts of the color pattern transcription factor *optix*. We further show that optix and the eyespot transcription factor spalt both bind to the promoter of *araucan*, suggesting that these two factors directly regulate *araucan.* Together, our data lead us to propose that *araucan* plays a specialized role in determining the hue of *J. coenia* wing scale iridescence and is directly regulated by core wing patterning transcription factors to modulate structural coloration.

KEYWORDS

structural coloration, butterfly wing patterns, gene regulatory network, evo-devo

INTRODUCTION

Butterfly wings have intricate color patterns that result from a combination of color pigmentation and scale structural interactions with light. Natural variations in color patterns and scale structures have motivated scientists to understand the genetic and molecular mechanisms that underlie the development and diversity of these patterns. In the last few years, a combination of new genomic resources and the ability to mutate genes using CRISPR-Cas9 has led to identification and functional validation of genes responsible for natural color pattern variation (Reed et al., 2011; Zhang, Mazo-Vargas, et al., 2017), (Nadeau et al., 2016; van der Burg et al., 2020), (Mazo-Vargas et al., 2017), (Ficarrotta et al., 2022), (Kunte et al., 2014; Rodriguez-Caro et al., 2021), (Westerman et al., 2018). In addition to mapping studies, homology with model insects such as *Drosophila melanogaster*, coupled with comparative transcriptomic studies, have highlighted additional color patterning genes (Carroll et al., 1994; Monteiro et al., 2013; Stoehr et al., 2013; Wee et al., 2022) (Matsuoka & Monteiro, 2018; Peng et al., 2020; Zhang, Martin, et al., 2017). Even though a number of wing patterning genes have been identified, however, we are still far from a comprehensive model of the color pattern formation process. In particular, our understanding of the genetic basis of structural coloration remains limited.

Here we investigate the role of the gene *araucan* in butterfly wing pattern development. In *D. melanogaster, araucan*, *caupolican*, and *mirror* are homeodomain proteins that belong to the *Iroquois* family of genes. Most ecdysozoans, including butterflies, have two *Iroquois* genes: one related to *mirror*, and one related to *araucan* and *caupolican*. *araucan* and *caupolican* appear to be the result of a duplication event at some point in the recent history of the lineage that includes *Drosophila* (Kerner et al., 2009). The *Iroquois* genes play multiple roles in *D. melanogaster* development, including regulating the pro-neural gene *achaete-scute* to form the notum, and specifying longitudinal wing veins by regulating *rhomboid* (Gómez-Skarmeta et al., 1996; Gómez-Skarmeta & Modolell, 1996; Ikmi et al., 2008). It was recently shown that *mirror* specifies a far posterior domain of butterfly wings – a function speculated to be ancestral in insects but lost in *D.*

melanogaster and other calypterate flies due to an evolutionary reduction in wing complexity (Chatterjee et al., in revision). We still know little about the role of the *araucan/caupolican* ortholog (hereafter *araucan*) in butterfly wings, however, except that whole-wing mRNA sequencing shows that it is expressed during wing development (Hanly et al., 2019; Hines et al., 2012). In this study we used knockout and expression approaches to investigate the wing patterning role of *araucan* in the common buckeye butterfly *Junonia coenia*. We found that this gene appears to play a specific function in regulating wing scale structure related to iridescence, and that knockouts have a pronounced effect on iridescence in the center of the eyespot.

MATERIALS AND METHODS

Phylogeny of *Iroquois* complex genes

We performed a reciprocal BLAST of *D. melanogaster Iroquois* complex genes *araucan*, *caupolican*, and *mirror* against the latest *J. coenia* and *Heliconius erato lativitta* genome sequences on lepbase.org (S.I. Appendix) to identify the orthologs in nymphalid butterflies. The amino acid sequences of the top hits JC_02265-RA, JC_02269-RA, HEL_009655-RA, and HEL_009656-RA were aligned to the *Iroquois* genes of *D. melanogaster* using MUSCLE (Edgar, 2004). We used these alignments to build a maximum likelihood gene phylogeny on IQ-TREE 2 (Minh et al., 2020) using ModelFinder (Kalyaanamoorthy et al., 2017) to estimate the best fit substitution model for our amino acid sequences. We used FigTree to visualize the tree.

CRISPR-Cas9 mutagenesis of *J. coenia araucan*

To assess the function of *araucan* in *J. coenia* we generated CRISPR-Cas9 somatic mosaic deletions targeting the *araucan* coding region. We used a previous protocol where early embryos are injected with single guide RNAs (sgRNAs) and Cas9 enzyme (Zhang, Mazo-Vargas, et al., 2017; Zhang & Reed, 2016). Since early embryos are syncytial, mutations are induced in a mosaic subset of cell lineages, resulting in mosaic knockout (mKO) animals (Zhang, Mazo-Vargas, et al., 2017; Zhang & Reed, 2016).

We designed two sgRNAs – 5'-CTGGGTACGATTTAGCAGCC-3' and 5'-CTCCTGCTCCTTGTCCTCGT-3' – to target the exon of *araucan* in *J. coenia* containing the conserved homeobox domain (Figure 1A). Possible off target sgRNAs were ruled out by blasting against the *J. coenia* genome assembly. sgRNAs were synthesized by Integrated DNA Technologies, Inc. (Coralville, IA, USA), rehydrated in 1x Tris-EDTA buffer, and mixed with Alt-R S.p. Cas9 Nuclease/Nickase (Integrated DNA Technologies, Inc., Coralville, IA, USA) to a final concentration of 200ng/ul sgRNA and 500ng/ul Cas9.

We collected eggs by placing leaves of *Plantago lanceolata* with gravid females for 1-2 hours, and then prepared eggs for microinjection by submersing them in 5% benzalkonium chloride (Sigma-Aldrich, St Louis, MO, USA) for 30s followed by a wash with distilled water. Prepared eggs were then lined up on double sided tape on glass slides and 2uL of the sgRNA / Cas9 mixture was injected into the eggs using 0.5-mm borosilicate needle (Sutter Instruments, Novato, CA, USA) and a PLI-100 Picoinjector (Harvard Apparatus, Holliston, MA, USA). Injections were completed within 2-3hrs after oviposition, and larvae from injected eggs were raised on artificial diet at 27°C, 70% humidity, and a 16hr : 8hr light : dark cycle. Adults were frozen upon emergence, and phenotyped and imaged using a Keyence VHX-7000 microscope.

Genotyping CRISPR mutants

We genotyped *J. coenia* mosaic knockout (mKO) mutants to confirm Cas9-induced deletions in *araucan*. We extracted DNA (OMEGA BIO-TEK, Norcross, GA, USA) from the thoracic flight muscles of butterflies that showed obvious wing pattern anomalies compared to wildtypes. We used PCR to amplify DNA from around the potential cut sites using the primers 5'-ATACTAAACCCTGCACCCGC-3' and 5'-ACGTACTCACAAGCGAACGT-3'. We ran amplified DNA from wildtype and mutant individuals on an agarose gel and purified (Monarch DNA Extraction and Purification kit, new England Biolabs, MA, USA) and cloned the PCR products into JM109 competent cells using pGEM®-T Easy Vector Systems (Promega Corporation, Madison, WI, USA). Transformed cells were amplified and Sanger sequenced at the Genomics Facility, Cornell Institute of Biotechnology, Ithaca, NY, USA.

Scanning electron microscope imaging of iridescent and wild type scales from *araucan* mKOs

We used scanning electron microscopy to assess structural differences between wild type and *araucan* mutant scales. Scales were cryofractured following a previous protocol (Ren et al., 2020). We then mounted whole scales and cryofractured scales of interest on carbon tape and sputter-coated them with an 8 nm layer of gold using a Cressington 208HR Sputter Coater. Images were acquired on an FEI Teneo LV SEM, using the Everhart-Thornley detector and beam parameters of 5.00 kV/6.3 pA with a 10-μs dwell time at the George Washington University Nanofabrication and Imaging Center (GWNIC), Washington, D.C, USA.

HCR fluorescent *in situ* hybridization of *araucan*

We used the coding sequence of *J. coenia araucan* to design a hybridization chain reaction (HCR) probe set. Specifically, we designed 8 pairs of 20bp probes (totaling 40bp per site) spanning the annotated *araucan* transcript (Table S1). BLAST analysis of the most recent *J. coenia* genome assembly confirmed no off-target binding sites existed for the *araucan* probe pairs. We dissected last instar larval imaginal discs and second day pupal wings, and used these to perform the HCR *in situ* hybridization as per Bruce et al. (dx.doi.org/10.17504/protocols.io.bunznvf6), with an Alexa 647 fluorophore, and counterstained with DAPI nuclear marker. For negative controls we performed the experiments without the *araucan* probes but with fluorophores. For positive controls we performed the experiment using previously published *wingless* probes, which show distinct wing margin and color pattern-related expression as previously described (Martin & Reed, 2010). Maturing scales of pupal wings are known to autofluoresce, especially in the green and orange wavelengths, so we took care to perform our pupal-stage HCR imaging in the far-red spectrum where we detected no significant autofluorescence in negative controls. We imaged *araucan*-stained wings on Leica Stellaris 5 confocal microscope in the laboratory of Dr. Eirene Markenscoff-Papadimitriou, Dept. of Molecular Biology and Genetics, Cornell University.

Chromatin immunoprecipitation and sequencing

We collected 40-44 last instar larval wings per replicate and 8-10 5 day old (~110 hours after pupation) pupal wings per replicate and fixed them in formaldehyde and glycine for chromatin immunoprecipitation sequencing (ChIP-seq), as previously described. (Lewis et al., 2016). Following the protocol of Lewis et al. (Lewis et al., 2019), 15-20µg of sheared DNA extracted from 5 day old pupal wing tissues wing discs was incubated overnight with rat anti-optix antibody as previously described (Lewis et al., 2019). A similar quantity of DNA was extracted from last instar larval wing tissue and incubated with rabbit anti-spalt polyclonal antibody (a gift from Dr. Michael Perry at the University of California, San Diego, USA). As a positive control for ChIP-seq, we used mouse anti-RNA-polymerase II antibody (ab5408; ABCAM, Boston, MA, USA) to bind to sheared DNA collected from last instar larval wing discs. As negative control, we incubated 2-5µg sheared DNA with equal volume of Dynabeads™ Protein A and Protein G (ThermoFisher Scientific Inc.). ChIP-seq libraries were prepared with a NEBNext DNA Ultra II kit following manufacturer recommendations, without performing size selection. Prepared libraries were sequenced by Biotechnology Resource Center (BRC) Genomics Facility (RRID:SCR_021727) at the Cornell Institute of Biotechnology on their Illumina NextSeq 500/550 platform using a read length of 2 x 32 bp, resulting in a read depth of approximately 20 milliion bp for the ChIP libraries and 30 million bp for negative controls. Sequencing reads were aligned to the “Version 2” genome of *J. coenia* available on lepbase.org and filtered and PCR duplicates removed following the pipeline previously described (Lewis et al., 2016; van der Burg et al., 2019). ChIP-seq peaks were called using MACS2 using q-value FDR of 0.05.

RESULTS

Identity of *Iroquois* family genes in *J. coenia*

We used *D. melanogaster* amino acid sequences of the *Iroquois* genes *araucan*, *caupolican*, and *mirror* to identify their orthologs in the most recent *J. coenia* and *H.*

erato lativitta genome assemblies. Our gene phylogeny confirmed previous results that there are three *Iroquois* genes in *D. melanogaster* and only two in Lepidoptera (Kerner et al., 2009), and that the *D. melanogaster araucan* and *caupolican* genes are products of a gene duplication that occurred after the split between Diptera and Lepidoptera (Figure 1B). JC_02265-RA of the v2 *J. coenia* genome assembly is the sister lineage of the *D. melanogaster araucan* and *caupolican* duo of paralogs. We hereafter refer to JC_02265-RA as *araucan* in *J. coenia*, but with the understanding that it is equally related to *caupolican*.

araucan knockouts result in iridescent blue scales via laminar thickening

We injected 596 eggs with Cas9 and *araucan* sgRNAs, of which 141 hatched and 92 survived to adulthood. Fourteen of the adults that emerged had wing pattern mutations. We observed two distinct classes of mutations, both of which involved iridescent coloration: (1) blue iridescence in mutant clones across the dorsal wing surface, and (2) a shift from purple to colorless specifically in eyespot foci (i.e., center spots). Genotyping confirmed that individuals from both mutant classes had lesions at the sgRNA sites in the *araucan* coding region (Figure S1).

Out of the fourteen mKO butterflies we observed, nine individuals showed mosaic clones of blue iridescence, exclusively on dorsal wing surfaces (Figure 1C, Figure S2). Since some naturally occurring populations of *J. coenia* occasionally have iridescent blue scales (Thayer et al., 2020) we assessed individuals from our wild type colony for similar iridescent scales. Out of the individuals randomly observed (n = 32), we did not observe any blue iridescent scales on the dorsal surface of the wings, which supports that the blue iridescence in the mKOs is a result of knockdown of *araucan* ($p < 0.005$, chi-square test). This conclusion was also supported by the fact that individuals with iridescent patches of scales presented this phenotype asymmetrically (Figure S2), consistent with cell linages mosaicism (Zhang, Mazo-Vargas, et al., 2017), whereas natural variation in iridescence is symmetrical.

We next wanted to identify what kind of structural changes in *araucan* mutant scales might underlie the increase in blue iridescence. Low magnification top-down electron micrograph images of wildtype and mKO scales showed no obvious

difference in scale ultrastructure (Figure S3). However, when we looked at coronal sections of the scales after cryofracturing, we noted that mutant scales had greatly increased basal laminar thickness compared to wild type (Figure 1C). This blue reflectance shift associated with thickening of the basal scale lamina has been previously described, and is consistent with the effect of *optix* knockouts in *J. coenia* (Thayer et al., 2020; Zhang, Mazo-Vargas, et al., 2017).

araucan **knockouts decrease iridescence in forewing eyespot foci**

Six of the *araucan* mKOs we recovered presented a striking phenotype that specifically affected the central foci of forewing eyespots. The scales at the center of the wild type *J. coenia* eyespot are unpigmented, and normally have a strong structural purple iridescent color (Figure 1D; Figure S4). In our *araucan* mutants, forewing eyespot foci largely lost their iridescence to become mostly colorless, with only some minor traces of violet or pink hue (Figure 1D, Figure S4). In all cases only scales in forewing eyespot foci were affected, although clear phenotypes were observed for both dorsal and ventral forewing eyespots (Figure 1D, Figure S4). Notably, the overall shape of the eyespot pattern itself always remained consistent and symmetrical between forewings, even though the mutant iridescence was asymmetric in all but two cases (Figure S4A). We observed no eyespot effects in hindwings.

araucan **is broadly expressed in nascent pupal scale cells**

Our mKOs demonstrate that *araucan* is necessary for normal structural coloration of *J. coenia* wing scales and appears to play a role in determining scale structure itself. Accordingly, we hypothesized that we should observe *araucan* expression in wings during scale morphogenesis. We additionally wanted to ask if there might be any detectable pattern-specific expression associated with the mutant phenotypes we observed, for example in eyespot foci. To characterize spatial transcription patterns of *araucan*, we used HCR *in situ* hybridizations targeting *araucan* mRNA in the developing last instar imaginal wing discs, at a stage right after the transcription factor spalt has established the domains for future eyespot development (1), and

early pupal wings, at a stage when scales are just beginning to elongate from scale precursor cells.

Our experiments did not reveal imaginal disc expression of *araucan*. They did, however, reveal broad *araucan* expression across pupal forewings and hindwings. Clear staining occurred in staggered rows of cells corresponding to the alternating cover and ground scale cells (Figure 2A). Three-dimensional confocal imaging revealed the highest levels of *araucan* transcripts localized to the apical extensions of nascent scales (Figure 2B). We did not observe spatial associations between *araucan* mRNA abundance and adult color patterns during early pupal wing development (data not shown). We cannot absolutely rule out color pattern associations at later stages of pupal development, however, because we cannot currently perform *in situ* hybridizations in mid- and late-stage wings due to challenges associated with probe penetrance and non-specific background signal in more mature scale cells. In any case, our *in situ* hybridizations are consistent with our knockout phenotypes in supporting a role for *araucan* specifically in wing scale development.

araucan **is a direct target of the optix and spalt transcription factors**

As described above, the *araucan* phenotypes we observed were reminiscent of *optix* knockout phenotypes, where blue structural coloration appeared in mutant clones in association with thickening of the basal lamina of scale cells (Figure 1C) (Thayer et al., 2020; Zhang, Mazo-Vargas, et al., 2017). The phenotypes differed, however, in that none of *araucan* mutants had obvious effects on pigmentation, whereas *optix* knockouts show a loss of ommochromes with replacement by melanins, in addition to structural color phenotypes. Because *araucan* mutants represented a subclass of *optix* knockout effects, we hypothesized that optix may achieve its structural coloration effects via regulation of *araucan*. To assess this possibility, we used ChIP-seq to examine the binding of the optix transcription factor at the *araucan* locus during wing development. Indeed, we found that optix binds to the *araucan* promoter, where it co-localizes with RNA polymerase II (Figure 3). Together, the knockout and ChIP-seq data suggest that optix is a direct positive regulator of *araucan*.

We were also curious about the highly specific effects of *araucan* on eyespot focus iridescence and hypothesized that it might be regulated by an eyespot determination factor. Therefore, as we did for optix, we used ChIP-seq to examine binding of the transcription factor spalt at the *araucan* locus. spalt is a key factor in the eyespot determination process – it is one of the earliest known genes to be expressed in the eyespot's focus in larval imaginal discs, and its expression is maintained in eyespot foci long into pupal development (Brunetti et al., 2001; Oliver et al., 2012; Stoehr et al., 2013; Wee et al., 2022; Zhang & Reed, 2016). We found that spalt binds to the *araucan* promoter, at the same location of optix and RNA polymerase II (Figure 3). This apparent regulatory interaction between the eyespot focus factor spalt and *araucan* provides a tentative model for how *araucan* can produce eyespot-specific phenotypes.

DISCUSSION

Here we used CRISPR-Cas9 knockouts to characterize the function of the *Iroquois*-complex gene *araucan* in butterfly wing pattern development. We found that it regulates two distinct aspects of structural iridescence in scale cells: (1) it represses blue iridescence across the dorsal wing surface, and (2) it promotes purple iridescence in forewing eyespot foci. While these effects may at first seem contradictory, they can both be achieved through a similar process: modulating the thickness of the scale cell basal lamina. For example, the switch from brown to blue we see in dorsal *araucan* mKO clones is achieved by an increase of laminar thickness. It is also conceivable that the switch of eyespot foci from purple to colorless, for example, is also achieved by similar changes in laminar thickness. We speculate a possible mechanism may be a simple linear shift along a brown-blue-violet continuum achieved via laminar thickening. While we need more data to test this model, we tentatively propose that *araucan* may play a negative role in regulating basal lamina thickness, such that knockouts result in increased thickness that may have different effects on color depending on the baseline thickness.

The *araucan* mKO phenotypes are visually dramatic and lead us to ask what kind of role *araucan* might play in butterfly wing pattern evolution. Our knockouts suggest that *araucan* has a very specific effect on scale cell lamina thickness, since

we didn't observe any other obvious pleiotropic effects. The lack of pleiotropic effects is interesting for two reasons. First, it suggests that its role in butterflies is significantly diverged from its role in *Drosophila*, where it has been duplicated, and the two duplicates serve numerous functions in cell field specification and wing vein development. Second, *araucan*'s specificity suggests that it may be well positioned to play a role in iridescent color pattern evolution. In this respect, it is likely important that the core color pattern development factors optix and spalt both bind to the *araucan* promoter. These apparent regulatory interactions provide and clear and plausible model for how both optix and spalt can modulate iridescence in specific color pattern elements, such as eyespots, through a downstream *araucan*-mediated scale structure pathway.

ACKNOWLEDGEMENTS

This work features the undergraduate thesis research of Kate Siegel, and we would like to thank the Cornell MBG-GGD honors thesis program participants for support and feedback on the project. We thank Dr. Eirene Markenscoff-Papadimitriou for use of her confocal microscope, and Dr. Michael Perry for his gift of spalt antibody. This work was supported by U.S. National Science Foundation GRFP DGE 2139899 to JMCM, by U.S. National Science Foundation grants IOS-2128164 and DEB-2242865 to RDR and Wilbur V. Harlan Research Fellowship for LSL.

REFERENCES

Brunetti, C. R., Selegue, J. E., Monteiro, A., French, V., Brakefield, P. M., & Carroll, S. B. (2001). The generation and diversification of butterfly eyespot color patterns. *Current Biology*, *11*(20), 1578-1585.

Carroll, S. B., Gates, J., Keys, D. N., Paddock, S. W., Panganiban, G. E., Selegue, J. E., & Williams, J. A. (1994). Pattern formation and eyespot determination in butterfly wings. *Science*, *265*(5168), 109-114.

Edgar, R. C. (2004). MUSCLE: a multiple sequence alignment method with reduced time and space complexity. *BMC bioinformatics*, *5*(1), 1-19.

Ficarrotta, V., Hanly, J. J., Loh, L. S., Francescutti, C. M., Ren, A., Tunström, K., Wheat, C. W., Porter, A. H., Counterman, B. A., & Martin, A. (2022). A genetic switch for male UV iridescence in an incipient species pair of sulphur butterflies. *Proceedings of the National Academy of Sciences*, *119*(3), e2109255118.

Gómez-Skarmeta, J.-L., del Corral, R. D., de la Calle-Mustienes, E., Ferrés-Marcó, D., & Modolell, J. (1996). Araucan and caupolican, two members of the novel iroquois complex, encode homeoproteins that control proneural and vein-forming genes. *Cell*, *85*(1), 95-105.

Gómez-Skarmeta, J. L., & Modolell, J. (1996). araucan and caupolican provide a link between compartment subdivisions and patterning of sensory organs and veins in the Drosophila wing. *Genes & development*, *10*(22), 2935-2945.

Hanly, J. J., Wallbank, R. W., McMillan, W. O., & Jiggins, C. D. (2019). Conservation and flexibility in the gene regulatory landscape of heliconiine butterfly wings. *Evodevo*, *10*(1), 1-14.

Hines, H. M., Papa, R., Ruiz, M., Papanicolaou, A., Wang, C., Nijhout, H. F., McMillan, W. O., & Reed, R. D. (2012). Transcriptome analysis reveals novel patterning and pigmentation genes underlying Heliconius butterfly wing pattern variation. *BMC genomics*, *13*(1), 1-16.

Ikmi, A., Netter, S., & Coen, D. (2008). Prepatterning the Drosophila notum: the three genes of the iroquois complex play intrinsically distinct roles. *Developmental biology*, *317*(2), 634-648.

Kalyaanamoorthy, S., Minh, B. Q., Wong, T. K., Von Haeseler, A., & Jermiin, L. S. (2017). ModelFinder: fast model selection for accurate phylogenetic estimates. *Nature methods*, *14*(6), 587-589.

Kerner, P., Ikmi, A., Coen, D., & Vervoort, M. (2009). Evolutionary history of the iroquois/Irx genes in metazoans. *BMC Evolutionary Biology*, *9*, 1-14.

Kunte, K., Zhang, W., Tenger-Trolander, A., Palmer, D., Martin, A., Reed, R., Mullen, S., & Kronforst, M. (2014). Doublesex is a mimicry supergene. *Nature*, *507*(7491), 229-232.

Lewis, J. J., Geltman, R. C., Pollak, P. C., Rondem, K. E., Van Belleghem, S. M., Hubisz, M. J., Munn, P. R., Zhang, L., Benson, C., & Mazo-Vargas, A. (2019). Parallel evolution of ancient, pleiotropic enhancers underlies butterfly wing

pattern mimicry. *Proceedings of the National Academy of Sciences*, *116*(48), 24174-24183.

Lewis, J. J., van der Burg, K. R., Mazo-Vargas, A., & Reed, R. D. (2016). ChIP-Seq-annotated Heliconius erato genome highlights patterns of cis-regulatory evolution in Lepidoptera. *Cell Reports*, *16*(11), 2855-2863.

Martin, A., & Reed, R. D. (2010). Wingless and aristaless2 define a developmental ground plan for moth and butterfly wing pattern evolution. *Molecular biology and evolution*, *27*(12), 2864-2878.

Matsuoka, Y., & Monteiro, A. (2018). Melanin pathway genes regulate color and morphology of butterfly wing scales. *Cell reports*, *24*(1), 56-65.

Mazo-Vargas, A., Concha, C., Livraghi, L., Massardo, D., Wallbank, R. W., Zhang, L., Papador, J. D., Martinez-Najera, D., Jiggins, C. D., & Kronforst, M. R. (2017). Macroevolutionary shifts of WntA function potentiate butterfly wing-pattern diversity. *Proceedings of the National Academy of Sciences*, *114*(40), 10701-10706.

Minh, B. Q., Schmidt, H. A., Chernomor, O., Schrempf, D., Woodhams, M. D., Von Haeseler, A., & Lanfear, R. (2020). IQ-TREE 2: new models and efficient methods for phylogenetic inference in the genomic era. *Molecular biology and evolution*, *37*(5), 1530-1534.

Monteiro, A., Chen, B., Ramos, D. M., Oliver, J. C., Tong, X., Guo, M., WANG, W. K., Fazzino, L., & Kamal, F. (2013). Distal-L ess Regulates Eyespot Patterns and Melanization in Bicyclus Butterflies. *Journal of Experimental Zoology Part B: Molecular and Developmental Evolution*, *320*(5), 321-331.

Nadeau, N. J., Pardo-Diaz, C., Whibley, A., Supple, M. A., Saenko, S. V., Wallbank, R. W., Wu, G. C., Maroja, L., Ferguson, L., & Hanly, J. J. (2016). The gene cortex controls mimicry and crypsis in butterflies and moths. *Nature*, *534*(7605), 106-110.

Oliver, J. C., Tong, X.-L., Gall, L. F., Piel, W. H., & Monteiro, A. (2012). A single origin for nymphalid butterfly eyespots followed by widespread loss of associated gene expression.

Peng, C. L., Mazo-Vargas, A., Brack, B. J., & Reed, R. D. (2020). Multiple roles for laccase2 in butterfly wing pigmentation, scale development, and cuticle tanning. *Evolution & Development*, *22*(4), 336-341.

Reed, R. D., Papa, R., Martin, A., Hines, H. M., Counterman, B. A., Pardo-Diaz, C., Jiggins, C. D., Chamberlain, N. L., Kronforst, M. R., & Chen, R. (2011). *optix* drives the repeated convergent evolution of butterfly wing pattern mimicry. *Science*, *333*(6046), 1137-1141. https://doi.org/10.1126/science.1208227

Ren, A., Day, C. R., Hanly, J. J., Counterman, B. A., Morehouse, N. I., & Martin, A. (2020). Convergent evolution of broadband reflectors underlies metallic coloration in butterflies. *Frontiers in Ecology and Evolution*, *8*, 206.

Rodriguez-Caro, F., Fenner, J., Bhardwaj, S., Cole, J., Benson, C., Colombara, A. M., Papa, R., Brown, M. W., Martin, A., & Range, R. C. (2021). Novel doublesex duplication associated with sexually dimorphic development of dogface butterfly wings. *Molecular biology and evolution*, *38*(11), 5021-5033.

Stoehr, A. M., Walker, J. F., & Monteiro, A. (2013). Spalt expression and the development of melanic color patterns in pierid butterflies. *EvoDevo*, *4*, 1-11.

Thayer, R. C., Allen, F. I., & Patel, N. H. (2020). Structural color in Junonia butterflies evolves by tuning scale lamina thickness. *Elife*, *9*, e52187.

van der Burg, K. R., Lewis, J. J., Brack, B. J., Fandino, R. A., Mazo-Vargas, A., & Reed, R. D. (2020). Genomic architecture of a genetically assimilated seasonal color pattern. *Science*, *370*(6517), 721-725.

van der Burg, K. R., Lewis, J. J., Martin, A., Nijhout, H. F., Danko, C. G., & Reed, R. D. (2019). Contrasting roles of transcription factors spineless and EcR in the highly dynamic chromatin landscape of butterfly wing metamorphosis. *Cell reports*, *27*(4), 1027-1038. e1023.

Wee, J. L. Q., Das Banerjee, T., Prakash, A., Seah, K. S., & Monteiro, A. (2022). Distal-less and spalt are distal organisers of pierid wing patterns. *Evodevo*, *13*(1), 1-14.

Westerman, E. L., VanKuren, N. W., Massardo, D., Tenger-Trolander, A., Zhang, W., Hill, R. I., Perry, M., Bayala, E., Barr, K., & Chamberlain, N. (2018). Aristaless controls butterfly wing color variation used in mimicry and mate choice. *Current Biology*, *28*(21), 3469-3474. e3464.

Zhang, L., Martin, A., Perry, M. W., van der Burg, K. R., Matsuoka, Y., Monteiro, A., & Reed, R. D. (2017). Genetic basis of melanin pigmentation in butterfly wings. *Genetics*, *205*(4), 1537-1550.

Zhang, L., Mazo-Vargas, A., & Reed, R. D. (2017). Single master regulatory gene coordinates the evolution and development of butterfly color and iridescence. *Proceedings of the National Academy of Sciences*, *114*(40), 10707-10712.

Zhang, L., & Reed, R. D. (2016). Genome editing in butterflies reveals that spalt promotes and Distal-less represses eyespot colour patterns. *Nature communications*, *7*(1), 11769.

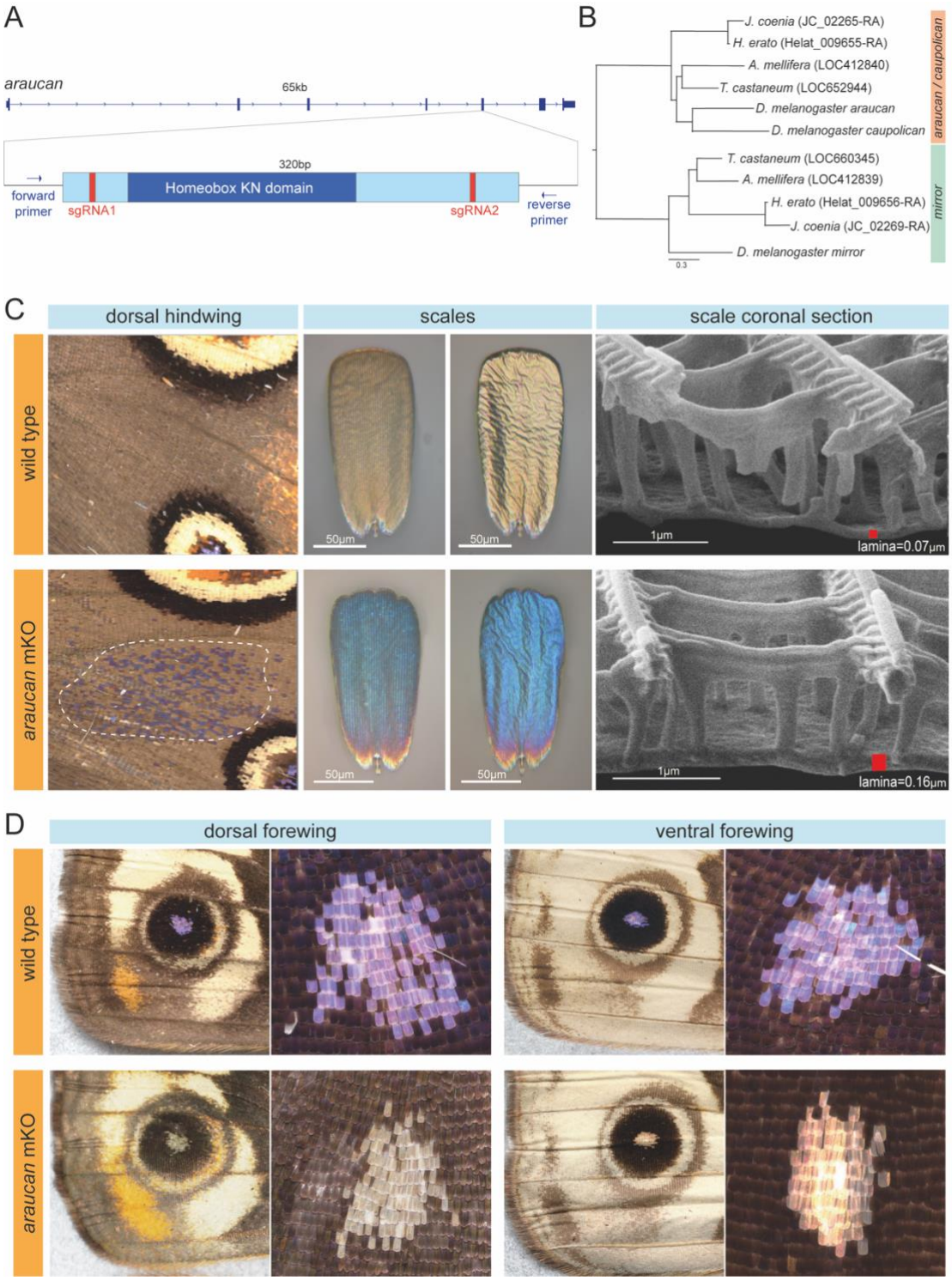
A
araucan
65kb
320bp
forward primer
sgRNA1
Homeobox KN domain
sgRNA2
reverse primer
B
J. coenia (JC_02265-RA)
H. erato (Helat_009655-RA)
A. mellifera (LOC412840)
T. castaneum (LOC652944)
D. melanogaster araucan
D. melanogaster caupolican
araucan / caupolican
T. castaneum (LOC660345)
A. mellifera (LOC412839)
H. erato (Helat_009656-RA)
J. coenia (JC_02269-RA)
D. melanogaster mirror
mirror
0.3
C
dorsal hindwing
scales
scale coronal section
wild type
araucan mKO
50µm
1µm
lamina=0.07µm
lamina=0.16µm
D
dorsal forewing
ventral forewing
wild type
araucan mKO

Figure 1. CRISPR-Cas9 knockouts of the *J. coenia araucan* gene have highly specific effects on wing scale iridescence. (A) Map of the *araucan* locus in *J. coenia,* annotated with the location of sgRNAs. The primers shown were used to validate deletions in mutants (Figure S1). (B) Maximum likelihood phylogeny of *J. coenia*, *H. erato lativitta*, *Tribolium castaneum*, *Apis mellifera*, and *D. melanogaster Iroquois* complex genes show that JC_02265-RA is the *araucan*/*caupolican* ortholog in *J. coenia* and JC_02269-RA is the ortholog of *mirror*. (C) Left panels: *araucan* mKO produces patches of blue iridescent scales. The top and bottom panels are from opposing wings of the same individual, illustrating mosaic asymmetry of the mutant. The wing figured on top has a wild type phenotype, while the wing figured on the bottom shows an apparent mutant patch with iridescence blue scales (white dashed line). Middle panel: Individual scales show wild type gold iridescent scales versus mutant blue iridescent scales from *araucan* mKO (left: abaxial; right: adaxial; scale bar: 50μm). Right panel: SEM of cryofractured scales show that wild type gold scales have thinner basal lamina (top) compared to mutant blue scales from *araucan* mKO (bottom). (D) *araucan* mKOs result in loss of purple iridescence in *J. coenia* eyespot foci. Top: Eyespot foci in wild type dorsal and ventral wings have purple iridescent scales. Bottom: *araucan* mKOs show loss of purple iridescence in both dorsal (left) and ventral (right) eyespot foci.

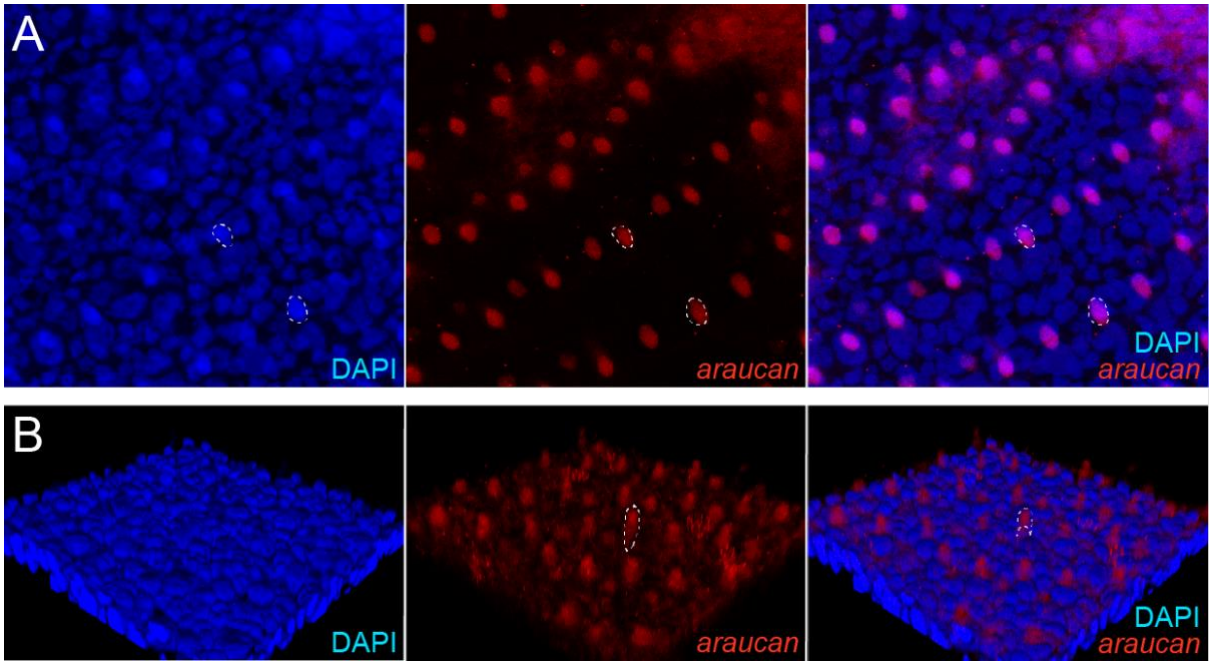

Figure 2. *araucan* transcripts are localized to the apical extensions of scale cells early in pupal development. (A) A planar confocal section of the HCR *in situ* hybridization shows *araucan* transcripts localized to parallel rows of nascent scale cells. The staggering of the scale cells represents the alternating ground (lower) and cover (overlapping) scales. (B) A three-dimensional reconstruction of pupal wing shows a high density of epithelial nuclei, marked by DAPI, with *araucan* transcript *in situ* hybridization signal enriched in the apical growth region of scale cells, which extend out from the epithelial surface. Exemplar cells are outlined by white dashed lines in order to compare positions between panels.

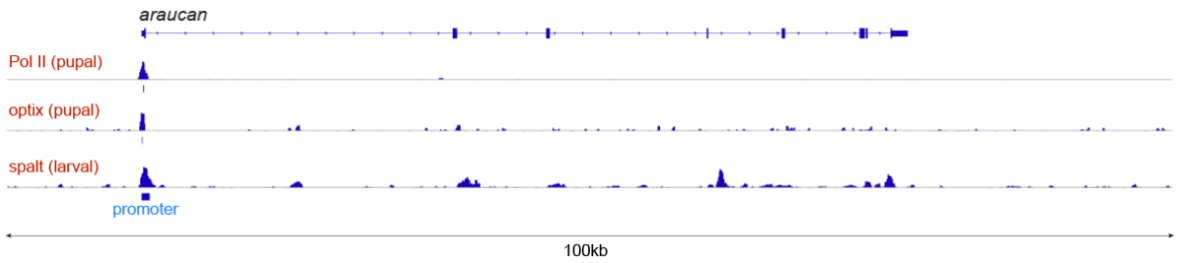

Figure 3. The color patterning transcription factors optix and spalt bind to the *araucan* promoter. ChIP-seq of RNA Polymerase II (Pol II) from pupal wings marks the promoter of the *araucan* gene. ChIP-seq of optix (pupal stage) and spalt (last instar imaginal discs) show signal at the same location, indicating that they bind to the *araucan* promoter.

Supporting Information

Table S1: HCR in situ hybridization probes for the *J. coenia araucan* transcript (JC_02265-RA). Green represents B1 initiator sequence.

Probes	Sequences (5'-3')
ara_p1_F	gAggAgggCAgCAAACggAAGGAGCTAATCTTCATCCGGCT
ara_p1_R	TGAGACTTCGAGATGACTCGGTAgAAgAgTCTTCCTTTACg
ara_p2_F	gAggAgggCAgCAAACggAAGGTGCGTCTATGTCTAAGCAC
ara_p2_R	AAACCATCAAGCAAAACCGGGTAgAAgAgTCTTCCTTTACg
ara_p3_F	gAggAgggCAgCAAACggAAGTATTGAGCGCCGGGGAAAC
ara_p3_R	CACGCAAGGATGCTGACCTCTAgAAgAgTCTTCCTTTACg
ara_p4_F	gAggAgggCAgCAAACggAAGGTATAGGCACTCCGCAGTC
ara_p4_R	CATATCTTCGGCTTGGACGCTAgAAgAgTCTTCCTTTACg
ara_p5_F	gAggAgggCAgCAAACggAATATTCCGTATCCGAGCAGCTG
ara_p5_R	ACCTCGCTTCGACTCTTCCTTAgAAgAgTCTTCCTTTACg
ara_p6_F	gAggAgggCAgCAAACggAATGGTCAACCTCACTTCTCGTC
ara_p6_R	AGCTTCGACCCGCACAATTATAgAAgAgTCTTCCTTTACg
ara_p7_F	gAggAgggCAgCAAACggAACGTACCCAGCACCATATCTGT
ara_p7_R	TTTCCGCCTGGCTGCTAAATTAgAAgAgTCTTCCTTTACg
ara_p8_F	gAggAgggCAgCAAACggAAAAGGGTTCTTCTTATGCTCGT
ara_p8_R	CTTCTCGCCTTTAGTCGGGTTAgAAgAgTCTTCCTTTACg

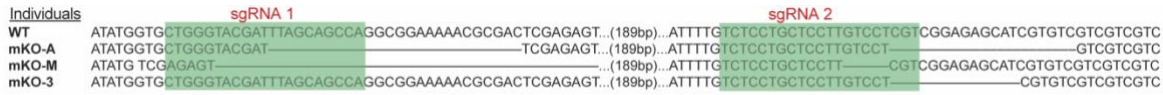

Figure S1. CRISPR-Cas9 targeting of *araucan* produces deletions at the sgRNA sites. Wild type and mutant sequences are shown. Green boxes indicate sgRNA binding sites. Knockouts mKO “A” and mKO “3” show dorsal iridescence phenotypes (Figure S2). mKO M has eyespot focus phenotype (Figure S4).

Figure S2. *araucan* mKOs displaying mutant patches of iridescent blue scales. Opposing wings from individual butterflies are shown to highlight the asymmetrical nature of the mosaic phenotypes.

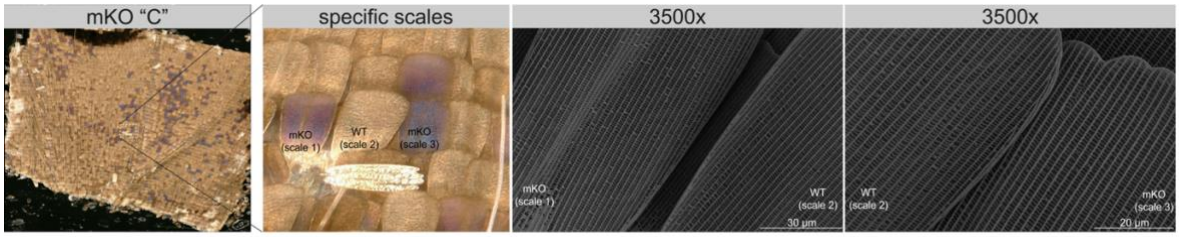

Figure S3. Top-down scanning electron micrographs of adjacent dorsal blue (mutant) and gold (wild type) scales from dorsal show no obvious gross differences in scale ultrastructure.

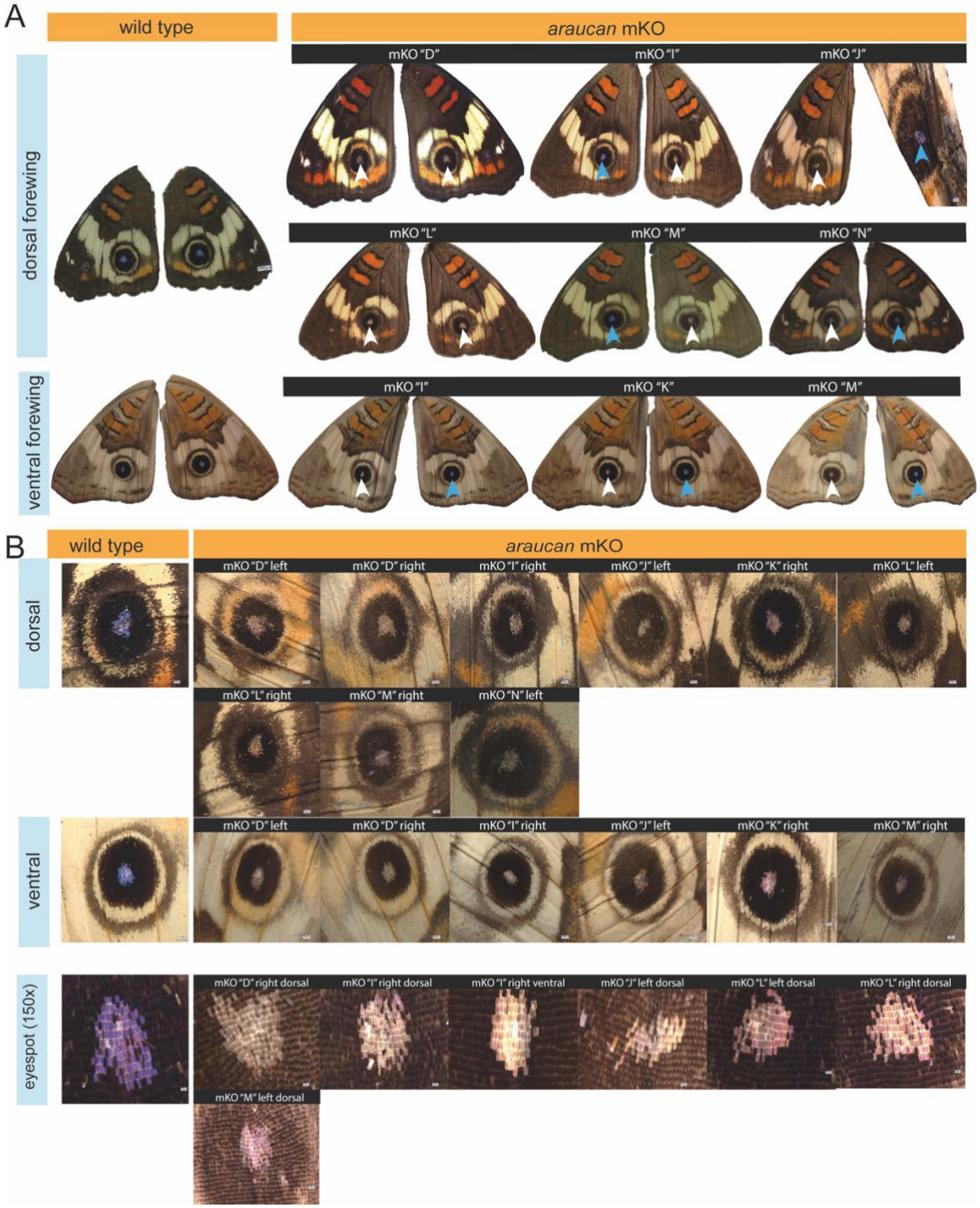
A
wild type
araucan mKO
dorsal forewing
mKO "D"
mKO "I"
mKO "J"
mKO "L"
mKO "M"
mKO "N"
ventral forewing
mKO "I"
mKO "K"
mKO "M"
B
wild type
araucan mKO
dorsal
mKO "D" left
mKO "D" right
mKO "I" right
mKO "J" left
mKO "K" right
mKO "L" left
mKO "L" right
mKO "M" right
mKO "N" left
ventral
mKO "D" left
mKO "D" right
mKO "I" right
mKO "J" left
mKO "K" right
mKO "M" right
eyespot (150x)
mKO "D" right dorsal
mKO "I" right dorsal
mKO "I" right ventral
mKO "J" left dorsal
mKO "L" left dorsal
mKO "L" right dorsal
mKO "M" left dorsal

Figure S4. *araucan* mKO results in loss of purple iridescence in *J. coenia* forewing eyespot foci. (A) Whole wing images of *araucan* mKOs displaying eyespot iridescence phenotypes. Both dorsal (top) and ventral (bottom) examples are illustrated. Eyespot foci phenotypes are annotated by arrowheads (blue: wild type eyespot foci; white: mutant eyespot foci). (B) High magnification images of dorsal (top) and ventral (bottom) *araucan* mKO eyespot effects.

Appendix 1

Iroquois-complex amino acid sequences from *Junonia coenia* (v2) and *Heliconius erato lativitta* (v1).

>JC_02269-RA (*mirror*)
MIRVLHRNKDSGRYMGAWSASECVRGREISCSLTLGQQPMAYLDFNYHGAFIGPP
VGGEACGGRSRPKLSEISSKSDYAIYACAHLKLYLNIEVLYGMDLNGARRKNATRET
TSTLKAWLNEHKKNPYPTKGEKIMLAIITKMTLTQDSGTGSSEDGDRPQQRLDLLG
QRTESEWSESRADSGPESPEPYERPIHPAYQHLPSRAPPGSTPASAKPRIWSLAD
MASKDGEAPAPPSAASAFYQSAAAAAARLAHPYGRPELYRGLYPPTHPADALLEYS
RSLALAAPAPAPPAPSPSSSSTSSLAEPPPPSRA

>JC_02265-RA (*araucan*)
DKIVFVNRYGAGYDLAARRKNATRESTATLKAWLNEHKKNPYPTKGEKIMLAIITKMT
LTQVSTWFANARRRLKKENKMTWEPKNKTDDDDDTMLSDEDKEQEDKIKTNKVIIM
PKFLTFSRFVIFHRRRKKECENVYGVIQKGREVRLTINCAGRSSHSAETSAEPRGES
GNAKMDEERKGDELLQGMHSQLLGYGIKEESKRGTSDCGVPIPASKPKIWSLADTA
ACKTPPPAAQPWPQHGYGPGPERSAAADGSSNGFALPATAAASPASGSYGRYGG
FPGAQYGGQHPCVHPAAFPDVQTDTPPQTPPNMKVPSVANPLGSGGGSGYCFPR
HQQSPQRDPYHNPHHANNHQPNQHHEGSAAFKPFYKRMRLNVSSPRLDWFGTF
FSFRPLCVNAAEGSGDTQIESNLAGLRFLVSRVEPASLLRPRLGTVGTITVAQCFPY
DQRSERFRCIVTSRDDSCNV

>Helat_009656-RA (*mirror*)
YGMDLNGARRKNATRETTSTLKAWLNEHKKNPYPTKGEKIMLAIITKMTLTQVSTWF
ANARRRLKKENKMTWEPRNRVDDDDNNNDDDDHKSNDGKDALDGKDSGTGSSE
DGERPQQRLDLLGQRTESEWSESRADSGPESPEPYERPLHPAYQHLPSRAPGST
PSAKPRIWSLADMASKDEATPPAVSFYQSAAARLAHPYRPELYRGLYPPSHPADVAL
LEYSRSLALAAPAPAPPAPSPSSSSTSSLADPPPRA

>Helat_009655-RA (*araucan*)
SNPYALKEGSGEMSAWTSAGLQPSGGYYPYDPTLAAYGYGAGYDLAARRKNATR
ESTATLKAWLNEHKKNPYPTKGEKIMLAIITKMTLTQVSTWFANARRRLKKENKMTW
EPKNKTDDDDDTMLSDEEKEQDDKIKPSKDDERKGDELLQGMHSQLLGYGIKEES
KRGTSDCGVPIPASKPKIWSLADTAACKTPPPAAQPWPQHGYGHGHERASAGDSN
SNGFALPATAAASPASGSYGRYGGFPGGQYGGQHPCVHPAAFPDVQTDTPPQTPP
NMKVPSVANPLGSGGGSGYCFPRHQQSPQRDLYHNPHHANNHQPNQHHEGSAA
FKPFYKRIVLRVKHEGAGSLLAVVTSSDDSGTVCSNL

1. R. D. Reed, J. E. Selegue, L. Zhang, C. R. Brunetti, Transcription factors underlying wing margin color patterns and pupal cuticle markings in butterflies. *EvoDevo* **11**, 1-10 (2020).